Journal of Molecular Liquids 221 (2016) 930–941

Contents lists available at ScienceDirect

Journal of Molecular Liquids

journal homepage: www.elsevier.com/locate/molliq

Fabrication of novel shape Cu and Cu/Cu_2O nanoparticles modified electrode for the determination of dopamine and paracetamol

Manoj Devaraj [a,d,**], R. Saravanan [b,*], RanjithKumar Deivasigamani [a], Vinod Kumar Gupta [c,e], F. Gracia [b], Santhanalakshmi Jayadevan [a]

[a] Department of Physical Chemistry, University of Madras, Maraimalai Campus, Guindy, Chennai 600 025, India
[b] Department of Chemical Engineering and Biotechnology, University of Chile, Beauchef 850, Santiago, Chile
[c] Department of Chemistry, Indian Institute of Technology Roorkee, Roorkee 247 667, India
[d] Department of Chemistry, School of Advanced Sciences, VIT University, Vellore 632014, India
[e] Department of Applied Chemistry, University of Johannesburg, Johannesburg, South Africa

ARTICLE INFO

Article history:
Received 8 March 2016
Received in revised form 24 May 2016
Accepted 7 June 2016
Available online 11 June 2016

Keywords:
Cyclic voltammetry
Paracetamol
Dopamine
Oleic acid
Differential pulse voltammetry

ABSTRACT

In this paper, we demonstrate and compare the synthesis of copper (Cu) and copper(I) oxide on Cu (Cu/Cu_2O) nanoparticles *via* thermal decomposition method using a combination of oleic acid and oleylamine and oleic acid alone. Using a combination of oleic acid and oleylamine, involves a single nucleation step and control in growth of nanoparticles produces high monodispersity in shape and protects the copper nanoparticles against oxidation. X-ray diffraction (XRD) confirms the formation of single phase Cu only and X-ray photoelectron spectroscopy (XPS) evidences the formation of Cu without any formation of oxides on surfaces for over a long period of time with good stability. In view of interest in electrochemical sensors, we explore the fabrication of a novel and highly sensitive electrode and compare the electrochemical current responses for simultaneous determination of paracetamol and dopamine using Cu/Cu_2O nanoparticles stabilized by oleic acid alone and Cu nanoparticles obtained from a combination of oleic acid and oleylamine. Interestingly, we observe that Cu/Cu_2O nanoparticles stabilized by oleic acid alone exhibit excellent electrochemical enhancement in the peak current response towards simultaneous determination of paracetamol and dopamine with an increase in peak-peak separation of 239 mV. Differential pulse voltammetry (DPV) studies show a linear response to dopamine within the concentration from 0.02 μM to 0.159 μM with a detection limit of 3.27 nM (S/N = 3).

1. Introduction

Metallic copper (Cu) nanoparticles have attracted attention as an important class of advanced material in the research field, because of its cost-effectiveness, and high electrical conductivity which is extensively used in electrical circuits [1]. Also, it has potential impact on photovoltaic cells [2], electrocatalyst in oxygen reduction reactions (ORR) [3] and in cancer cell killings and germicides [4]. In general, copper nanoparticles are found to oxidize at room temperature in the absence of strong protecting/stabilizing agents [5]. To synthesize copper nanoparticles, there are wide range of methods reported in the literature which include: reverse micelles [6], microemulsion [7], sonochemical [8], chemical vapour condensation [9], radiolytic reduction [10], laser irradiation [11] electrodeposition [12] and chemical reduction [13]. The synthesis of copper nanoparticles under room temperature is more attractive for commercial applications, but it mostly involves precious reagents and reducing agents for attaining oxygen free environment. Surprisingly, the synthesis of Cu nanoparticles using conventional reduction methods lack in the stability of Cu nanoparticles and can be easily oxidized in aqueous medium when H_2O molecules exist in the reaction conditions [14]. However it is well known that the electronic structure and physical properties of the nanoparticles depend upon the composition of the atoms present within the nanoparticles [15,16]. Therefore, the formation of surface oxide under ambient conditions in copper nanoparticles resulting in the conversion of Cu^0 to Cu_2O (Cu^+)/CuO (Cu^{2+}) and it was found to lose/alter their physical and optical properties of Cu nanoparticles.

The major challenge in the above methods lies in the difficulty to control the shape and size of the nanoparticles which highly suffers from particle agglomeration and hence it results in broad size distribution [17]. One way is to overcome the surface oxidation of copper nanoparticles with homogenous particle distribution *via* a successful thermal decomposition method by introducing organic surfactant (fatty acids) like oleic acid and oleylamine which minimizes the oxidation susceptibility of the material. Park et al. [18] had first put forward for the ultra-large scale synthesis of monodisperse metal nanocrystals involving

* Corresponding author.
** Correspondence to: M. Devaraj, Department of Chemistry, School of Advanced Sciences, VIT University, Vellore 632014, India.
E-mail addresses: manojdvrj@gmail.com (M. Devaraj), saravanan3.raj@gmail.com (R. Saravanan).

http://dx.doi.org/10.1016/j.molliq.2016.06.028
0167-7322/

metal oleate complex in presence of high boiling solvent 1-octadecene. Zhong and coworkers reported size controlled synthesis of Cu nanoparticles using oleic acid (alone), only mixture of shape morphology was produced [19]. Considering this difficulty, much more effort has been focused on the synthesis of monodisperse metallic Cu nanoparticles involving completely protected Cu nanoparticles. This is because, the properties of nanoparticle depend only on the shape and dimensions and hence it is significant goal of this research work. Sun et al. [20] proposed a method for the synthesis of FePt nanoparticles involving thermal decomposition of platinum acetylacetonate in presence of oleic acid and oleylamine resulting in the formation of monodisperse nanoparticles with control in shape and size. There are numerous reports existing on the synthesis of metal/metal oxide nanoparticles protected by oleic acid alone [21] however, combination of oleic acid and oleylamine protected nanoparticles has been proved to be an effective protective agent in non-aqueous medium [22,23]. Taking into consideration of previous reported literatures, much attention has been focused in the present work for the synthesis of well-defined Cu nanoparticles using in combination of oleic acid and oleylamine as capping agents in order to control the growth and shape of nanoparticles. However, there are no reports available on the synthesis, comparison of the surface properties of monodisperse Cu nanoparticles using various protecting agents like oleic acid alone and also in mixture of oleic acid and oleylamine. Hence, in this work, we synthesis and compare the surface morphology of copper nanoparticles using different protecting agents such as oleic acid alone and also mixture of oleic acid and oleylamine are undertaken.

Usage of dopamine and paracetamol above the therapeutic levels can cause a variety of adverse side effects, and therefore in order to monitor the concentration levels of dopamine and paracetamol is of high demand [24]. Since dopamine and paracetamol coexist in human fluids, the simultaneous determination is essential to protect the human health from critical dangerous diseases [25]. The major problem in the electrochemical determination of dopamine is the interference from other redox active species present which may undergo electrolysis at a similar potential to that required to oxidize or reduce the desired target molecule [26]. As a result overlapping of voltammetric response has been observed for mixture of analytes. This has to overcome by the use of various nanocomposites modified electrode having excellent conductivity and catalytic properties with minimal surface fouling effect make them suitable for the simultaneous determination of dopamine and paracetamol than conventional GC electrodes [27,28]. Among the various metal nanocomposites reported on the modified electrodes, dispersion of Cu nanostructures on multiwalled carbon nanotubes (MWCNTs) are favored because it potentially provides more active sites which may show some interesting synergistic properties that are different from MWCNTs [29] or Cu nanostructures alone [30]. This effect results in fast electron rate transfer with good peak-peak separation, reduce overpotential and high reproducibility with increase in sensitivity and selectivity.

The nanoparticles obtained from oleic acid alone and in combination of oleic acid and oleylamine were dispersed on acid functionalized MWCNTs decorated on glassy carbon (GC) electrode and compare the electrochemical behavior for the simultaneous determination of paracetamol and dopamine. The electrochemical measurements are carried out using cyclic voltammetry and differential pulse voltammetry with satisfactory results are observed.

2. Experimental

2.1. Chemicals and instrumentation

Copper acetate monohydrate [$Cu(CH_3COO)_2 \cdot H_2O$], oleic acid, oleylamine, 1,2,3,4-Tetrahydronaphthalene (anhydrous, 99%), dibenzyl ether (>98%), *tert*-butylamine borane complex (97%), 1-octadecene (90%) were purchased from Sigma-Aldrich. Sodium hydroxide, hexane, ethanol and acetone were obtained from Merck. MWCNTs of length (L = 20–30 nm) with an outer diameter of 1–2 nm and wall thickness of about 0.5–2 μm was purchased from Sigma-Aldrich. Acid functionalization of MWCNTs was carried out with concentrated HNO_3 and H_2SO_4 in a ratio of 1:3, then sonicate the reaction mixture for 30 min and centrifuged at 8000 rpm resulting in formation of high purity –COOH functionalized MWCNTs [31]. 0.1 M Phosphate buffer (pH-7.0) solution (PBS) was prepared with Na_2HPO_4 and NaH_2PO_4 was used as supporting electrolyte. All chemicals and reagents used in the experiments were of analytical grade and used without further purification. All the solutions were prepared using double distilled (DD) water.

All the electrochemical measurements were performed on PGSTAT-12 electrochemical work station, (AUTOLAB, The Netherlands BV) controlled by general purpose electrochemical system (GPES). The measurements were based on a three electrode system, with a glassy carbon (GC) electrode of geometric area (0.07 cm^2), being used as a working electrode, a Pt wire in the form of a spiral with high geometrical surface area (~20 cm^2) was used as a counter electrode and saturated calomel electrode (SCE) as the reference electrode. Prior to each experiments, GC surface was polished with increasingly finer grade alumina powders (1, 0.3 and 0.05 μm) down to mirror polish, sonicated for about 15 min in DD water, degreased with acetone and washed with copious amount of DD water. All the solutions were purged with analar grade nitrogen for at least 30 min prior to each electrochemical measurement and a nitrogen environment was maintained throughout the experiments.

FT-IR spectra were recorded for pure oleic acid, oleylamine and Cu nanoparticles stabilized by oleic acid and oleylamine as KBr pellets using BRUKER (TENSOR 27) in the region 4000–400 cm^{-1} with the resolution of 4 cm^{-1}. The morphology of the Cu nanoparticles was observed by utilizing a TECNAI-G^2 (model T-30) S-twin high resolution transmission electron microscope (HRTEM) operated at an accelerating voltage of 300 kV. X-ray diffraction (XRD) results were collected by using BRUKER D8 advance X-ray diffractometer with monochromatic Cu Kα radiation (λ = 1.5418 Å). XPS measurements were carried out in an ultra high vacuum (UHV) chamber (evacuated to 3.5×10^{-10} mbar) of the photoelectron spectrometer Omicron Nanotechnology, Germany (GmbH) equipped with a monochromatic X-ray source (AlKα, hv = 1486.6 eV). The binding energy of the samples was calibrated by setting the C1s peak to 284.6 eV. The peaks were deconvoluted by means of a standard CasaXPS software (v.2.3.13; product of CasaXPS Software Ltd., U.S.A.) to resolve the separate constituents after background subtraction. The chemical state of each element was identified by comparing the binding energy obtained after de-convolution with the standard values available in the hand book of XPS [32].

2.2. Sample preparation of dopamine and paracetamol

Stock solution (0.01 M) of dopamine (i/v) was prepared using 0.1 M PBS from the obtained i/v solution of dopamine (DOMIN-40 mg/mL) of pharmaceutical formulations. From the stock solution, the required dopamine volumes are siphoned out and used for further experimental studies. 400 mg paracetamol per tablet, obtained from local drug store of paracetamol pharmaceutical formulations is accurately weighed and crushed with mortar and pestle until a finer and homogeneous powder resulted. The obtained powdered tablets are dispersed in 100 mL standard flask with 0.1 M PBS (pH-7.0) and the resulted mixture was sonicated for 10 min and filtered using Whatmann filter paper and the obtained solution was diluted to the required concentrations.

2.3. Synthesis of copper-oleate complex

The synthesis method reported in the literate was adopted [18] in which 4.8 g of sodium hydroxide (120 mM) was dissolved in mixture of 50 mL of DD water and 80 mL of ethanol under nitrogen atmosphere with constant stirring. To the stirring reaction mixture, 40 mL of oleic

acid (120 mM) was added dropwise and the pH was adjusted to 7.0. 10 mL of $Cu(OAc)_2$ (40 mM) dissolved in water was added into the reaction mixture and few minutes later 40 mL hexane was added and the resulting solution was heated to 60 °C and maintain at this temperature for 4–5 h. After the end of the reaction, reaction mixture in which the uppermost organic layer containing copper-oleate was washed with distilled water and separated using separating funnel. After the separation of aqueous layer, the organic layer containing hexane was evaporated *via* roto-evaporator resulting in the formation of copper-oleate complex.

2.4. Synthesis of copper nanoparticles using oleic acid

In a typical reaction, the asprepared copper-oleate complex (obtained from above step) was dissolved in 40 mL of 1-octadecene and the reaction mixture was heated to 110 °C and kept at this temperature for 15 min under nitrogen (N_2) atmosphere. At this point, water molecules present in the reaction mixture get removed during the progress of the reaction and then further increase the reaction temperature to 180 °C with an increase in the heating rate of 5 °C/min. The reaction temperature was cooled to room temperature and the resultant brown Cu nanoparticles were precipitated out with 500 mL of ethanol and centrifuged at 7000 rpm, finally dried in vacuum oven at 60 °C.

2.5. Synthesis of Cu nanoparticles with combination of oleic acid and oleylamine

Copper acetate [3 mM, 0.544 g] was mixed with 5 mL dibenzyl ether and 5 mL tetralin in 100 mL round bottomed flask with continuous streaming of N_2 atm. After complete dissolution, 1.5 mL of each oleic acid (5 mM) and oleic amine (5 mM) was added into the reaction mixture. These are followed by the addition of (10 mM, 0.869 g) *tert*-butylamine borane complex dissolved in 0.1 mL oleic acid and oleylamine containing 0.5 mL tetralin was added into the reaction mixture. The reaction temperature was increased to 120 °C, and maintained at this temperature for 20 min for the complete removal of water molecules present. After 20 min, the reaction temperature was further increased to 180 °C with an increase in the heating rate of 5 °C/min. The significant color change from deep blue to brown indicates the formation of Cu nanoparticles. The reaction temperature was allowed to cool at room temperature and the resultant products are washed three times with 100 mL mixture of ethanol and hexane, centrifuged at 7000 rpm and dried in vacuum oven at 60 °C.

2.6. Electrode fabrication

1 mg of carboxyl functionalized MWCNTs was dispersed in 1 mL of (0.5%) ethanolic nafion solution by sonication for 30 min to get homogeneous black suspension [33]. Each of 1 mg/1 mL of the asprepared Cu nanoparticles obtained [using oleic acid alone (dispersed in ethanol) and combination of oleic acid and oleylamine are dispersed in hexane] are mixed into MWCNTs dispersion, stirred under room temperature and further kept at ultrasound treatment for 15 min. The fabrication procedure of the modified electrode has been performed by casting 5 μL of Cu-MWCNTs dispersion on GC electrode surface and allowing to dry under ambient conditions. The modified electrode was washed with several copies of PBS before use.

3. Results and discussion

3.1. XRD and XPS characterization

Fig. 1A shows the typical XRD pattern of Cu/Cu_2O nanoparticles obtained from stabilization with oleic acid alone. The nanoparticles are found to be crystallized into *face-centered cubic* (*fcc*) structure with the corresponding diffraction peaks appeared at 43.34°, 50.36° and 74.09° can be indexed as (111), (200) and (220) planes of Cu (JCPDS card No. 01-089-2838) which are comparable with those earlier reported [34]. Surprisingly, it can be seen (Fig. 1A), that in addition to the Cu peaks we have observed the diffraction peaks at 36.47°, 42.32°, 61.40° and 73.50° which are indexed as (111), (200), (220) and (311) planes corresponding to Cu_2O (JCPDS card No. 01-078-2076) indicating that Cu_2O molecules coexist with Cu in the product. Moreover, the diffraction peak intensity ascribed to Cu_2O is found higher when compared to Cu, which indicates that more extends of Cu_2O formation is favored by the presence of oleic acid stabilized Cu nanoparticles. Meanwhile, the surface of Cu phase was oxidized into Cu_2O this suggests that possibility for the oxidation (crystalline phase transition) is more [35]. This behavior may lead to instability of the product and hence results in distorted spherical morphology.

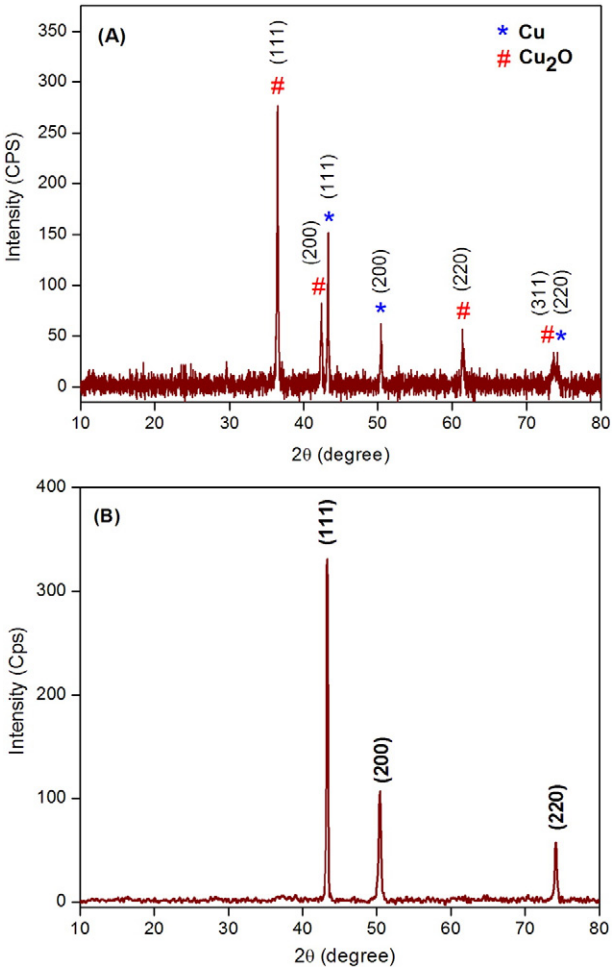

Fig. 1. XRD spectra of Cu/Cu_2O and Cu nanoparticles stabilized by (A) oleic acid alone and (B) combination of oleic acid and oleylamine.

In order to overcome some of the drawbacks, extensive efforts have been put into the synthesis of copper nanoparticles stabilized by both oleylamine and oleic acid with high stability. Fig. 1B shows the XRD pattern obtained from stabilization of both oleylamine and oleic acid. The diffraction peaks appeared at 43.38°, 50.46° and 74.16° can be indexed as (111), (200) and (220) planes of face centered cubic Cu phase (JCPDS card No. 01-085-1326). Therefore, XRD diffraction analysis confirms the formation of single phase Cu alone. It is quite interesting that, combination of oleylamine (as cosurfactant) and oleic acid provides an effective stabilization and also it prevents further oxidation of copper nanoparticles which results in high stability of the products obtained. Furthermore, there is no observation of any Cu_2O and CuO diffraction

peaks which confirms the formation of high purity copper nanoparticles only.

XPS provides information about the chemical compositions of Cu nanoparticles stabilized by oleic acid alone and in combination of oleic acid and oleylamine. Fig. 2 shows the typical XPS spectra of (A) Cu 2p (B) Auger of Cu nanoparticles stabilized by oleic acid alone. From the survey spectrum, the sample synthesized is composed of Cu, O and C only, where the carbon and oxygen peaks are attributed to the residual carbon (sample itself) and adventitious hydrocarbon (instrument itself) respectively. The Cu 2p line peaks are fitted using Gaussian-Lorentzian fitting procedure from which Cu $2p_{1/2}$ and Cu $2p_{3/2}$ peaks were observed. The appearance of splitting in two peaks of Cu $2p_{3/2}$ region (Fig. 2A) which indicates that Cu nanoparticle consists of two phases of Cu (two valence states) [36].

The deconvolution of two main core-level Cu $2p_{3/2}$ peak regions was resolved and the peak positions located at 930.15 eV and 931.79 eV correspond to the presence of Cu^0/Cu^+. There is no observation of any satellite peaks which confirms the absence of any CuO or $Cu(OH)_2$ present in the sample [32]. In addition, the core-level peak-peak difference between Cu $2p_{1/2}$ and Cu $2p_{3/2}$ regions is of 19.85 eV which confirms the presence of Cu^0/Cu^+ only. In general, the main peaks observed for Cu^0/Cu^+ regions cannot be distinguishable because the binding energy values are very close to each other. Therefore to confirm the presence of different valence states (close binding energy values) of the sample present in the surface, we can determine only from the peak positions of LMM-2 Auger transitions. From the LMM-2 Auger spectrum (Fig. 2B), we confirm the peak position at 569.0 eV corresponds to the presence of elemental Cu only [37]. But, the relative percentage of Cu-Cu_2O is Cu 22.37 (%) and Cu_2O 77.63 (%) respectively. Hence, in presence of oleic acid the Cu nanoparticles may get oxidized more predominantly into Cu_2O. Therefore, it may be concluded that the Cu nanoparticles are oxidized to Cu_2O from the surface, and the presence of CuO is negligible.

Considering the synthesis of single phase of copper nanoparticles, and in order to remove the surface oxidation of copper nanoparticles we implement the synthesis of copper nanoparticles in combination of oleic acid and oleylamine. Fig. 2C shows the typical XPS spectra of Cu 2p region of copper nanoparticles stabilized by combination of oleic acid and oleylamine. From survey scan, it confirms that the as prepared Cu nanoparticle consists of Cu, C and O only. Fig. 2C shows the core-level signals of Cu 2p and the peaks are fitted using Gaussian fitting procedure and the peak positions are deconvoluted into Cu $2p_{3/2}$ and Cu $2p_{1/2}$. The Cu $2p_{3/2}$ core-level (main peak) peak positions could be fitted with the two components centered at 932.29 eV and 934.61 eV may be attributed to Cu^0 (or Cu^+) and Cu^{2+} [(CuO or $Cu(OH)_2$] respectively. The shake-up lines are significant in core-level spectrum, from which it is possible to determine the presence of Cu^0/Cu^+ or Cu^{2+} in the sample. In general for Cu^{2+}, it is accompanied with the presence of satellite peaks (appears when the outgoing photoelectron simultaneously interacts with a valence electron and excites it to a higher-energy level) with respect to the main peak for d^9 configuration in Cu^{2+}. In the case of Cu^0/Cu^+, the d-shell configuration is completely filled (d^{10}), hence the screening effect *via* charge transfer into the d-levels are not possible and hence the absence of satellite peak (Fig. 2C). Moreover, the peak-peak difference between Cu $2p_{3/2}$ (932.29 eV) and Cu $2p_{1/2}$ (952.12 eV) is $\Delta = 19.83$ eV also reveals the presence of metallic Cu only (as evidence from XRD). Taking into consideration of the measurement of XPS, the formation of small degree of surface oxidation/

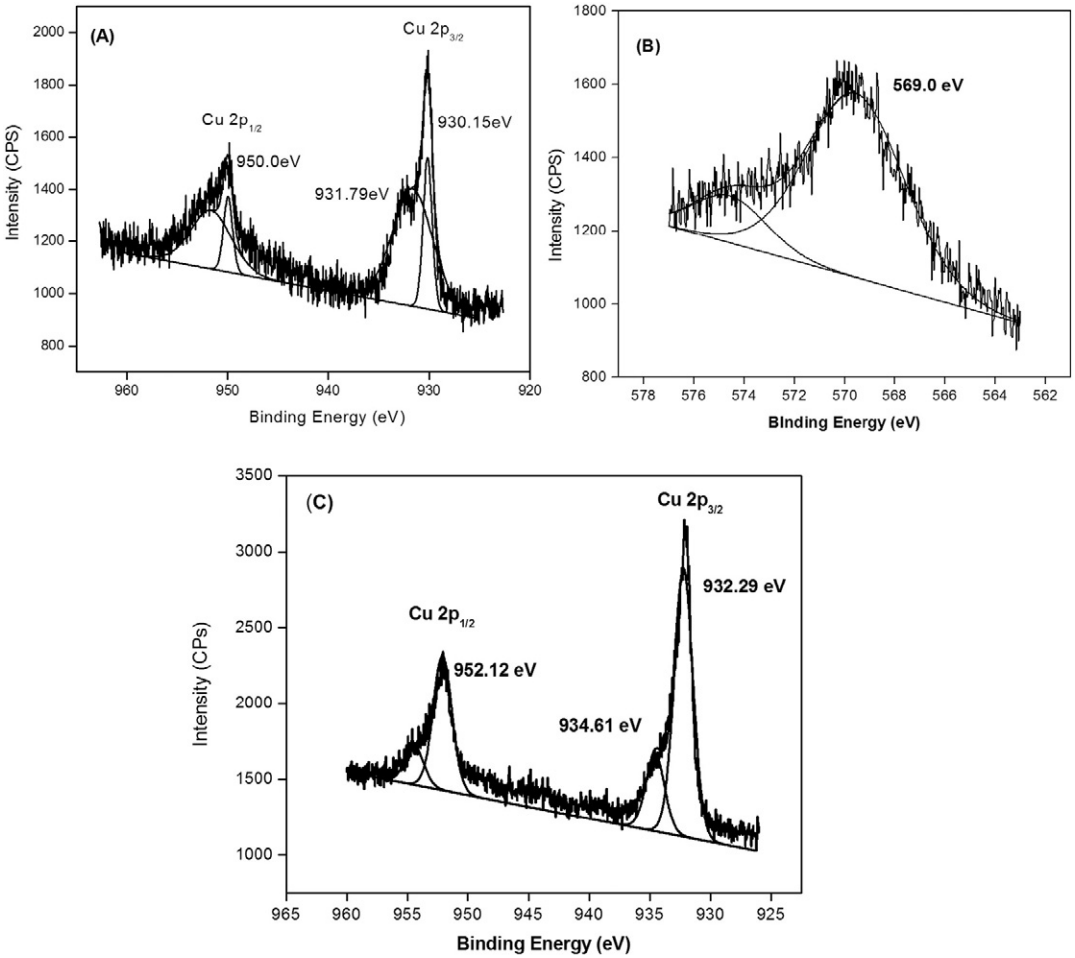

Fig. 2. XPS spectra of (A) Cu 2p and (B) Auger of Cu/Cu_2O nanoparticles and (C) Cu 2p of Cu nanoparticles stabilized by oleic acid alone and combination of oleic acid and oleylamine.

hydration cannot be prevented using this method which cannot be detected by XRD. Therefore the peak position for Cu $2p_{1/2}$ observed at 934.61 eV is due to the presence of lower amount of $Cu(OH)_2$ when the sample becomes exposed in air containing humidity. The relative percentage of Cu nanoparticles obtained using in combination of oleic acid and oleylamine is Cu 77.57 (%) and $Cu(OH)_2$ 22.43 (%) respectively. Hence, it revealed that Cu nanoparticles are formed more predominantly than $Cu(OH)_2$, using in combination of oleic acid and oleylamine.

3.2. Morphological characterization

Fig. 3(A and B) shows the HRTEM images obtained from stabilization of pure oleic acid alone stabilized Cu nanoparticles. During initial stages of the formation of Cu nanoparticles, copper-oleate complex reacts with 1-octadecene, the color of the reaction mixture was found to be blue and increasing the reaction temperature to 120 °C, and then it was allowed to remain at this temperature for 20 min. After approximately 20 min, the reaction temperature was further increased to 180 °C and then the color changes from blue to dark brown, with continued aging the reaction mixture at 180 °C, Cu nanoparticles are formed. As evidence from Fig. 3(A and B), in which the particles are found to be distorted spherical shape together with a thin outer layer on each particle surface was observed, which reflects that few nanometers layer thickness of thin Cu_2O was formed on the surface of each copper nanoparticles as evidence from XRD results.

This oxide formation is explained in such a way that, due to the oxophilicity and the generation of free carboxyl groups [38,39] on the surface of the Cu nanoparticles oxidation is induced, and hence a halo type formation on the surface of the nanoparticles resulted. The average particle diameter of the oleic acid stabilized Cu nanoparticles is calculated to be 340 ± 20 nm. Moreover, the synthesis of copper nanoparticles using pure oleic acid in presence of high boiling point solvent 1-octadecene mainly suffers from procedures of separation [40] and purification of copper nanoparticles from the reaction mixture (low yield) and hence it results in aggregation leading to distorted morphology. Therefore in this synthesis method, the surface oxidation of copper nanoparticles is rapid and hence more intense diffraction peaks are observed for Cu_2O in XRD and XPS.

3.3. Solvent effect

Regarding the need for control of experiments, in the synthesis of Cu nanoparticles the solvent plays an imperative role during the course of the reaction for large scale synthesis. For solvent dependent synthesis of Cu nanoparticles, the solvent having withstanding properties at higher boiling point and also much easier to separate from the reaction mixture is of higher demand [41]. Most of the methods reported using octyl ether (a highly expensive solvent) to maintain stability at higher temperature [42–44]. In this context under optimum experimental conditions, combination of dibenzyl ether and tetralin can be an alternative for this typical synthesis method and maintain the reaction temperature in a narrow range. By choosing either dibenzyl ether or tetralin alone does not form any homogenous of the reactant molecules because $Cu(CH_3COO)_2$ mainly suffers from solubility particularly in organic medium. Therefore in combination of dibenzyl ether and tetralin was chosen and it provides superior solubilizing medium for the reactant molecules and may lead to all the reactant molecules gets involved in the reaction (homogeneous). In general, as the boiling point of the solvent increases, the reactivity of the molecules also increases which results in increase in diameter of the particle size with homogeneity [45]. With all the above considerations, we have chosen the combination of dibenzyl ether and tetralin as solvent in this typical method of synthesis.

By taking the above beneficiary factors, the combination of both oleic acid and oleylamine provides control over shape and growth of Cu nanoparticles. Fig. 3(C and D) displays the HRTEM images obtained from the synthesis of copper nanoparticles in combination of oleic

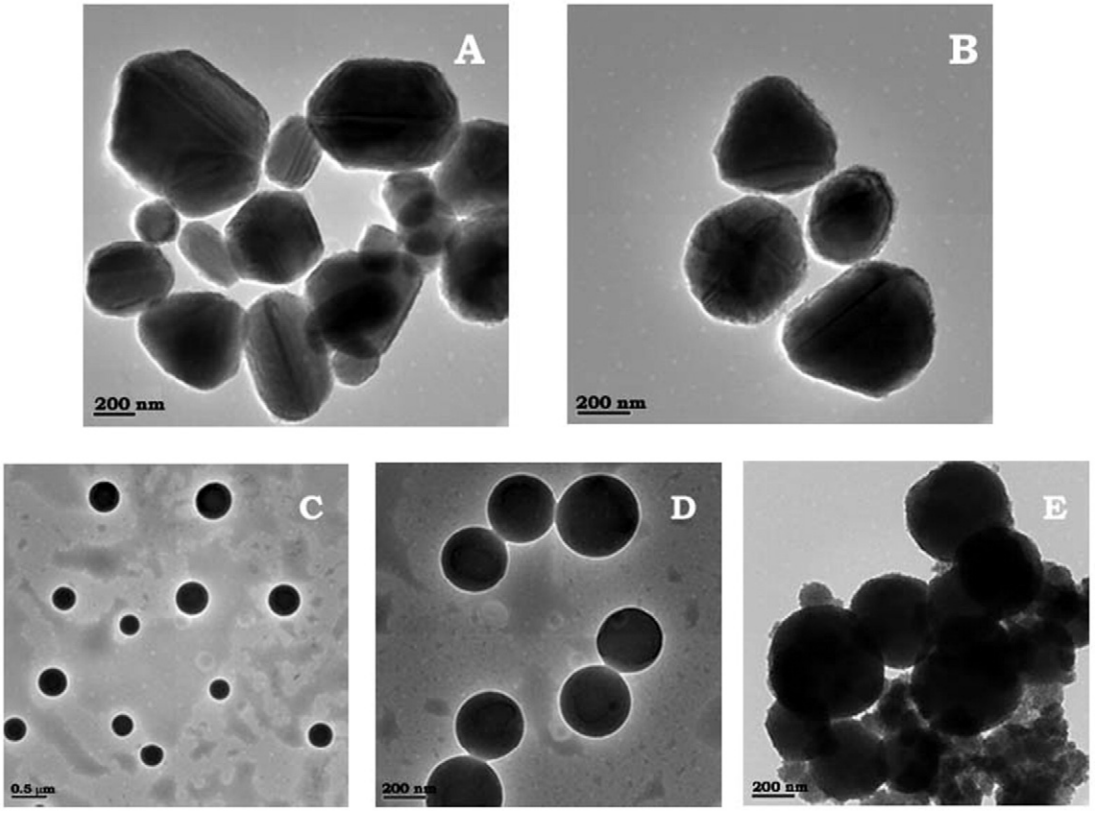

Fig. 3. HRTEM images of (A and B) Cu/Cu_2O nanoparticles stabilized by oleic acid alone, (C and D) Cu nanoparticles using combination of oleic acid and oleylamine and (E) oleylamine alone.

acid and oleylamine. The procedure adopted in this typical method is the synthesis of monodisperse Cu nanoparticles using in combination of oleic acid and oleylamine *via* one-pot reaction. The significant part of this method of synthesis is that dibenzyl ether (bp-297 °C) and tetralin (bp 207 °C) are used as solvents instead of 1-octadecene, to withstand high temperature during the thermal decomposition without any morphological defects and retained the products (easy to separate) in large scale with good yield. It can be clearly seen that, significant improvements are observed when Cu nanoparticles are synthesized in combination of oleic acid and oleylamine in which monodisperse with well-defined spherical surface morphology [46]. In order to obtain the homogeneous and shape controlled synthesis of metal nanoparticles, it was found that reducing agents play an important role for the reduction of metal ions, by choosing weak reducing agents like amine-borane complex which slower the reducing rate of Cu^{2+} rather than strong reducing agents [47] like ($NaBH_4$), that prevails in control over size of Cu nanoparticles. Hence in the present work for the synthesis of Cu nanoparticles in combination with oleic acid and oleylamine using *tert*-butylamine borane complex (having mild/weaker reducing ability) offers much more advantageous, which slower the reducing rates of Cu cations which is clearly observed from the significant color change of Cu^{2+} color from deep blue to blue and then to brown. This step-by-step change in the color is the significant role of reducing agents for the slower reducing rate which results in monodispersity. In the same time, the presence of oleylamine alone (having weak reducing ability) causing multi-nucleation step [46] and does not offer much more control over growth and shape of monodisperse nanoparticles (Fig. 3E).

For optimizing stoichiometric molar ratios of oleic acid and oleylamine used for the synthesis of Cu nanoparticles, control of experiments for various mole ratios of oleic acid and oleylamine was carried out. It was found that, well defined monodisperse spherical Cu nanoparticles are obtained only for equimolar ratio (1:1) of oleic acid and oleylamine. This observation emphasis that formation of $–COO^-$ in the oleic acid molecules and $–NH_3^+$ in the oleylamine molecules in equal proportion in the mixture. In all the other remaining mixture compositions, excess of –COOH and $–NH_2$ groups coexist that creates the formation of highly polydisperse with distorted and irregular shapes. Therefore, equimolar ratio (1:1) of oleic acid and oleylamine was selected for the synthesis of Cu nanoparticles.

The observation of uniform and monodisperse shape oriented synthesis of copper nanoparticles using oleic acid and in combination of co-surfactant oleylamine under hydrothermal reaction conditions has been explained as follows: Under optimized reaction conditions, oleic acid is first added into the reaction mixture (having –COOH group in the oleic acid) does not have a strong tendency towards the binding of Cu nanoparticles [48] as Cu nuclei earlier generated during the reaction mixture. Hence after the addition of oleic acid (after 1 min), oleylamine (equi-molar ratio 1:1) is added into the reaction mixture, which generates carboxylate anion having preferential binding and hence suppresses the growth of copper nanoparticles (single nucleation step). At the same time, the protonation of oleylamine increases, the preferential binding of carboxylate anion also get increased and hence more and more carboxylate anions binds the Cu metal ions which results in stability of copper nanoparticles. Therefore, the obtained copper nanoparticles are of uniform shape and size with high purity Cu nanoparticles (single phase) as evidenced from XRD and XPS. The average particle diameter of the Cu nanoparticles is calculated to be 285 ± 5 nm. This is explained as, due to the presence of additional oleylamine which influences the kinetics for the Cu nanoparticles formation and it controls the morphological parameters and hence it results in monodispersity.

3.4. Mechanism

When oleylamine is added to the oleic acid, the carboxyl acid groups present in the oleic acid are partially deprotonated into carboxylate anions [46,49]. It is well known that carboxylate anions having high electron donating ability, capable of preferential binding with Cu ions more effectively. In other words, the possibility for the formation of hydrogen bonding gets reduced as the formation of carboxylate anion (Scheme 1). Therefore in conclusion, combination of oleic acid and oleylamine for stabilization of copper nanoparticle provides more stable and favor the formation of monodisperse Cu nanoparticles.

FTIR spectroscopy (Fig. 4) was carried out to investigate the molecular interactions between pure oleic acid, oleylamine and in combination of oleic acid and oleylamine stabilized Cu nanoparticles. The spectra shows the FTIR of pure oleic acid in which the peaks obtained at 2855 cm^{-1} and 2926 cm^{-1} are due to the presence of symmetric and asymmetric stretching vibrations of $–CH_2$ modes. A strong peak observed at ~1711 cm^{-1} corresponds to the characteristic stretching vibrations of C═O and weak band at 2672 cm^{-1} for –OH stretching vibrations of the dimerized acid [50]. In the case of oleylamine, the peak observed at 1562 cm^{-1} and 3320 cm^{-1} corresponds to the NH_2 scissoring mode and N—H stretching vibrations respectively [51].

For the Cu nanoparticles stabilized by the combination of oleic acid and oleylamine $–CH_2$ symmetric and asymmetric stretching vibrations appeared at 2853 cm^{-1} and 2923 cm^{-1} confirms that oleyl group gets adsorbed on Cu nanoparticles effectively. Moreover the C═O stretching frequency vibration mode of –COOH group and the observation of NH_2 stretching vibration is negligible which confirms that the absence of free –COOH and $–NH_2$ groups on the surface of Cu nanoparticles. Furthermore, the $–COO^-_{(asymm)}$ and $–COO^-_{(symm)}$ stretching vibrations appeared at $–COO^-_{(asymm)}$ ~1563 cm^{-1} and $–COO^-_{(symm)}$ ~1387 cm^{-1} respectively. The appearance of shoulder peak at ~1623 cm^{-1} can be attributed to the antisymmetric deformation of the $–NH_3^+$ group. From this observation we suggest that all oleic acid (–COOH) and oleylamine ($-NH_2$) molecules are deprotonated into $–COO^-$ anions and $–NH_3^+$ cations which forms an acid-base complex gets involved in the reaction for the stabilization of Cu nanoparticles.

3.5. Electrochemical determination of paracetamol and dopamine

Fig. 5A compares the cyclic voltammograms of bare GC (black line), MWCNTs (red line), Cu-OA-OM/MWCNTs (pink line) and Cu/Cu_2O-OA/MWCNTs (blue line) modified GC electrodes in presence of 0.1 mM dopamine containing 0.1 M PBS at a scan rate of 50 mV s^{-1}. It can be clearly seen that bare GC electrode does not show any significant response throughout the potential range from 0 to +0.4 V in presence of dopamine. Whereas, MWCNTs modified GC electrode shows a pair of well-defined redox peak with an anodic peak potential (E_{pa}) +0.179 V and cathodic peak potentials (E_{pc}) +0.118 V with increase in the peak currents when compared to bare GC electrode. Furthermore, the oxidation peak current (I_{pa}) of dopamine at MWCNTs modified GC electrode is increased by 5.0 fold than the bare GC electrode which reflects that, MWCNTs modified GC electrode favors the oxidation of dopamine. Moreover, the oxidation current obtained at MWCNTs modified GC electrode for dopamine gets decreased for continuous and repeated of over 5 cycles. This may be due to the adsorption effect of dopamine at MWCNTs surface which results in electrode fouling effect caused by the oxidation products of dopamine [52]. While Cu-OA-OM/MWCNTs/GC modified electrode also shows a redox peak with an anodic peak potential (E_{pa}) +0.186 V and cathodic peak potentials (E_{pc}) +0.106 V with decrease in the redox peak currents and the oxidation potential of dopamine is shifted to more positive region. A considerable shift in the peak potentials for the oxidation of dopamine at Cu-OA-OM/MWCNTs/GC modified electrode, was due to stabilization of long aliphatic chains on Cu nanoparticles causes the Cu nanoparticles on the modified surface to be immiscible in the aqueous solution, and hence the oxidation potential for dopamine get slightly shifted towards more positive potential with decrease in peak current due to hydrophobicity.

It is quite interesting when compared to bare GC, MWCNTs/GC and Cu-OA-OM/MWCNTs/GC electrode, Cu/Cu_2O-OA/MWCNTs modified

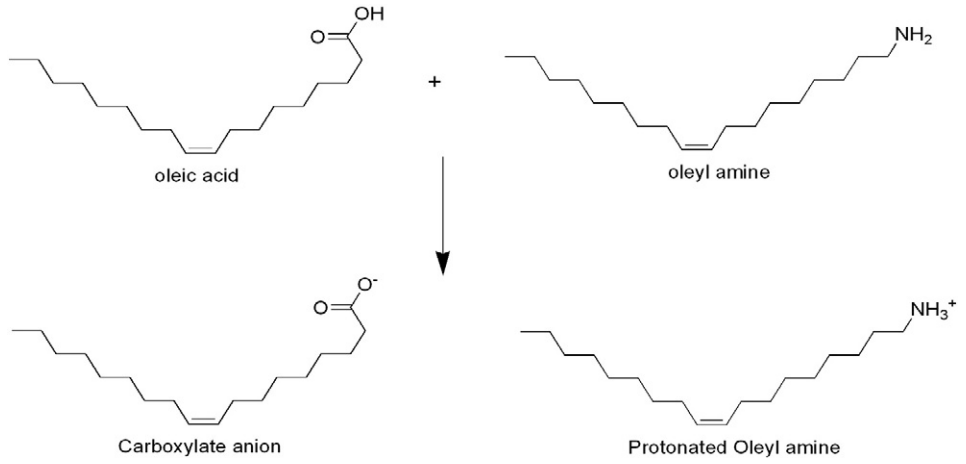

Scheme 1. Mechanism for stabilization of copper nanoparticles in combination of oleic acid and oleylamine.

GC electrode shows a drastic increase in the redox peak current response with anodic peak potential (E_{pa}) + 0.237 V and cathodic peak potentials (E_{pc}) + 0.110 V. The oxidation peak current (I_{pa}) of dopamine at Cu/Cu_2O-OA/MWCNTs modified GC electrode are of 2.37, 4.19 and 12.11 fold higher than MWCNTs/GC, Cu-OA-OM/MWCNTs/GC and bare GC respectively. Also the oxidation of dopamine at Cu/Cu_2O-OA/MWCNTs modified GC electrode starts oxidation at 74.17 mV which is 29.83 mV and 39.83 mV lesser than MWCNTs/GC (104 mV) and Cu-OA-OM/MWCNTs/GC modified electrode (114 mV). This enhancement in the peak current and less positive starting oxidation potential at CuO-OA/MWCNTs modified GC electrode is explained in such a way that in combination of MWCNTs and CuO nanoparticles (dispersed in ethanol, hydrophilic) facilitates the electron transfer rate between the electrode surface, which significantly improves the catalytic oxidation of dopamine.

Fig. 5B compares the cyclic voltammograms of bare GC (black line), MWCNTs (red line), Cu-OA-OM/MWCNTs (pink line) and Cu/Cu_2O-OA/MWCNTs (blue line) modified GC electrodes in presence of 0.1 mM paracetamol containing 0.1 M PBS at a scan rate of 50 mV s^{-1}. The bare GC electrode does not possess any significant electrochemical activity within the entire potential sweep range. When utilizing MWCNTs on GC electrode, it shows a pair of well-defined redox peak with an anodic peak potential (E_{pa}) + 0.369 V and cathodic peak potentials (E_{pc}) + 0.291 V with increase in the peak currents when compared to bare GC electrode. Similarly as observed for dopamine, MWCNTs modified GC electrode undergoes electrode fouling effects caused by the oxidation products of paracetamol which results in decrease in

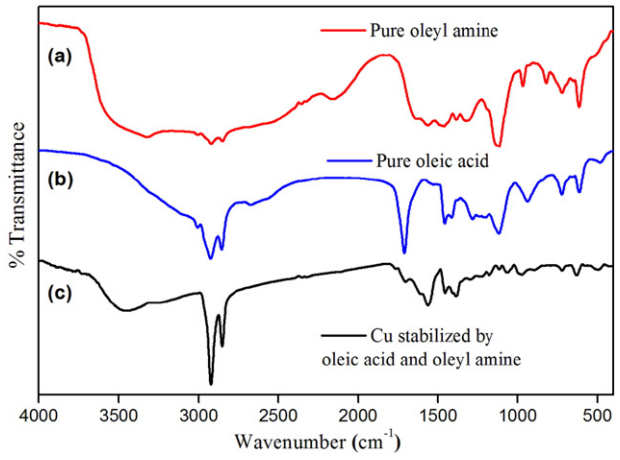

Fig. 4. FT-IR spectra of pure oleic acid, pure oleylamine and Cu nanoparticles stabilized by combination of oleic acid and oleylamine.

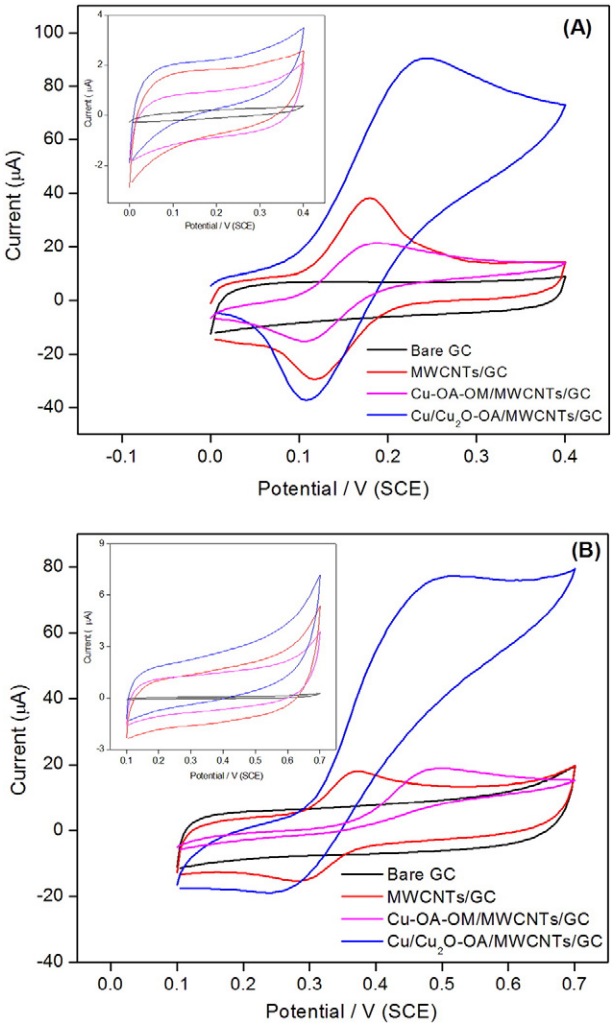

Fig. 5. (A) Cyclic voltammograms for 0.1 mM dopamine in 0.1 M PBS (pH 7.0) on Cu/Cu_2O-OA/MWCNTs/GC (blue line), Cu-OA-OM/MWCNTs/GC (pink line), MWCNTs/GC (red line) modified electrodes and bare GC (black line) at a scan rate of 50 mV s^{-1}. (B) Cyclic voltammograms for 0.1 mM paracetamol in 0.1 M PBS (pH 7.0) on Cu/Cu_2O-OA/MWCNTs/GC (blue line), Cu-OA-OM/MWCNTs/GC (pink line), MWCNTs/GC (red line) modified electrodes and bare GC (black line) at a scan rate of 50 mV s^{-1}.

peak current response for continuous of over 5 cycles. Furthermore, the oxidation peak current (I_{pa}) of paracetamol at MWCNTs modified GC electrode is increased by 2.34 fold higher than the bare GC electrode which reflects that, MWCNTs modified GC electrode favors the oxidation of paracetamol. However we observe an irreversible peak at Cu-OA-OM/MWCNTs/GC modified electrode, with the appearance of anodic peak ($E_{pa} = +0.485$ V) with decrease in peak current response is due to the presence of hydrophobic effect on Cu nanoparticles makes it not feasible for electrochemical oxidation of paracetamol in physiological medium.

When compared to bare GC, MWCNTs/GC and Cu-OA-OM/MWCNTs/GC modified electrode, Cu/Cu_2O-OA/MWCNTs modified GC electrode shows a strong increase in the peak current for paracetamol with anodic peak potential (E_{pa}) +0.475 V and cathodic peak potentials (E_{pc}) = +0.262 V. The obtained peak current for paracetamol at CuO-OA/MWCNTs modified GC electrode was highly stable for continuous of over 5 cycles, which reflects that in combination of MWCNTs and Cu/Cu_2O nanoparticles has anti-electro fouling activity caused by the oxidation products of paracetamol which results in high stability of the modified electrode [53]. This confirms that CuO nanoparticles stabilized by oleic acid alone exhibits higher electrocatalytic activity towards paracetamol than Cu-OA-OM/MWCNTs/GC, MWCNTs/GC and bare GC effectively.

3.6. Simultaneous determination of dopamine and paracetamol using CV

Simultaneous determination of dopamine and paracetamol is essential in order to investigate the complications from overlapping of other oxidizing species on electrode surfaces. Since paracetamol, ascorbic acid and uric acid coexist in the same oxidation potential and it mainly suffers from above mentioned interfering compounds which are more or less close to the oxidation potential of dopamine which results in peak overlapping and hence reduces selectivity [54]. Therefore simultaneous determination of dopamine and paracetamol is of higher importance in this present work.

Fig. 6 compares the cyclic voltammograms of MWCNTs/GC (red line), Cu-OA-OM/MWCNTs/GC (pink line) and Cu/Cu_2O-OA/MWCNTs (blue line) modified GC electrode in presence of mixture of 0.1 mM dopamine and paracetamol at a scan rate of 50 mV s^{-1}. As can be seen from Fig. 6, MWCNTs modified GC electrode shows a pair of redox peaks in presence of dopamine and paracetamol with anodic peak potential (E_{pa}) appeared at +0.174 V and cathodic peak potential (E_{pc}) at +0.135 V for dopamine while for paracetamol with anodic (E_{pa} = +0.377 V) and cathodic (E_{pc} = +0.296 V) peak potentials respectively. Whereas, Cu-OA-OM/MWCNTs/GC modified electrode shows two merged broad redox peaks and convolution for simultaneous determination in mixture of dopamine and paracetamol, which reflects that Cu nanoparticles stabilized by combination of oleic acid and oleylamine does not favors simultaneous determination in mixture of pharmaceutical samples. In contrast to MWCNTs/GC, Cu-OA-OM/MWCNTs/GC modified electrode, Cu/Cu_2O-OA/MWCNTs modified GC electrode shows a large enhancement in the redox peak currents with anodic peak potential (E_{pa}) appeared at +0.242 V and cathodic peak potentials (E_{pc}) appeared at +0.094 V for dopamine while for paracetamol with anodic peak potential (E_{pa}) +0.481 V and cathodic peak potentials (E_{pc}) +0.284 V respectively. In addition the oxidation peak current (I_{pa}) of dopamine and paracetamol at Cu/Cu_2O-OA/MWCNTs/GC modified electrode are increased by 3.42 and 4.80 fold higher than MWCNTs/GC electrode while it was increased by 5.46 and 5.49 fold greater than Cu-OA-OM/MWCNTs/GC modified electrode respectively. When compared with MWCNTs/GC modified electrode, Cu/Cu_2O-OA/MWCNTs modified GC electrode starts oxidation of dopamine at 66 mV while for MWCNTs/GC modified electrode it starts oxidation at 122 mV with a difference of 56 mV, which indicates that CuO nanoparticles having more reactive sites and accelerates the oxidation of dopamine to reach the electrode surface faster, and as consequence oxidation becomes easier.

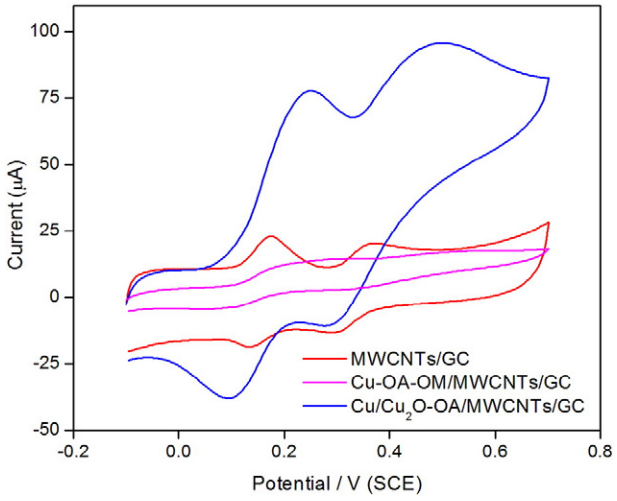

Fig. 6. Cyclic voltammograms for mixture of 0.1 mM dopamine and 0.1 mM paracetamol in (0.1 M PBS -pH 7.0) Cu/Cu_2O-OA/MWCNTs/GC (blue line), Cu-OA-OM/MWCNTs/GC (pink line), MWCNTs/GC (red line) modified electrodes at a scan rate of 50 mV s^{-1}.

In general, the high peak separation between analytes of the anodic potential values is required to quite enough for the simultaneous determination of analytes, and hence results in well-distinguishable peak values makes suitable for determination in mixture of analytes [55]. By considering the facts, as in Fig. 6 Cu/Cu_2O-OA/MWCNTs modified GC electrode shows a peak-peak separation between dopamine and paracetamol of the anodic potential value of [E_{pa} (DA) = +0.242 - E_{pa} (PA) = +0.481] 239 mV which is higher than MWCNTs modified GC electrode of [E_{pa} (DA) = +0.174 - E_{pa} (PA) = +0.377] 203 mV. Hence Cu/Cu_2O-OA/MWCNTs modified GC electrode offers 36 mV higher than MWCNTs/GC modified electrode which makes effective for simultaneous determination of dopamine and paracetamol. Thus the higher peak separation values between dopamine and paracetamol of the anodic peak potential, coupled with the increased peak current which provides a fascinating material for the determination of dopamine and paracetamol simultaneously (Scheme 2).

3.7. Effect of scan rate

In order to understand the nature of electrocatalytic process, the effect of scan rate on the electrocatalytic oxidation of paracetamol has been studied on the Cu/Cu_2O-OA/MWCNTs modified GC electrode. Fig. 7A shows the CVs of Cu/Cu_2O-OA/MWCNTs modified GC electrode in 0.1 M PBS containing 0.01 mM dopamine with different scan rates (from inner to outer) of (a) 10 (b) 20 (c) 30 (d) 40 (e) 50 (f) 60 (g) 70 (h) 80 (i) 90 (j) 100 mV s^{-1}. With increase in the scan rate the peak current increase linearly and the potential was shifted to more positive potentials. The peak current was proportional to the square root of scan rate over a range of 5 to 100 mV s^{-1} and calibration plot of ip *versus* $\nu^{1/2}$ as seen in Fig. 7B gives reasonable straight lines passing through origin which means that electrocatalytic reduction of dopamine at Cu/Cu_2O-OA/MWNCTs modified GC electrode is under diffusion controlled [56]. The linear regression equation can be expressed as:

$$I_{pa}\ (\mu A) = -18.54 + 12.08\nu^{1/2}\ (\text{mV s}^{-1}), R^2 = 0.998 \quad (1)$$

It is further confirmed by linear relationship (Fig. 7C) between $\log(\nu)$ and $\log(i_{pa})$ with a slope of 0.6 which is close to the theoretical value of 0.5 indicating the electron transfer is under diffusion controlled

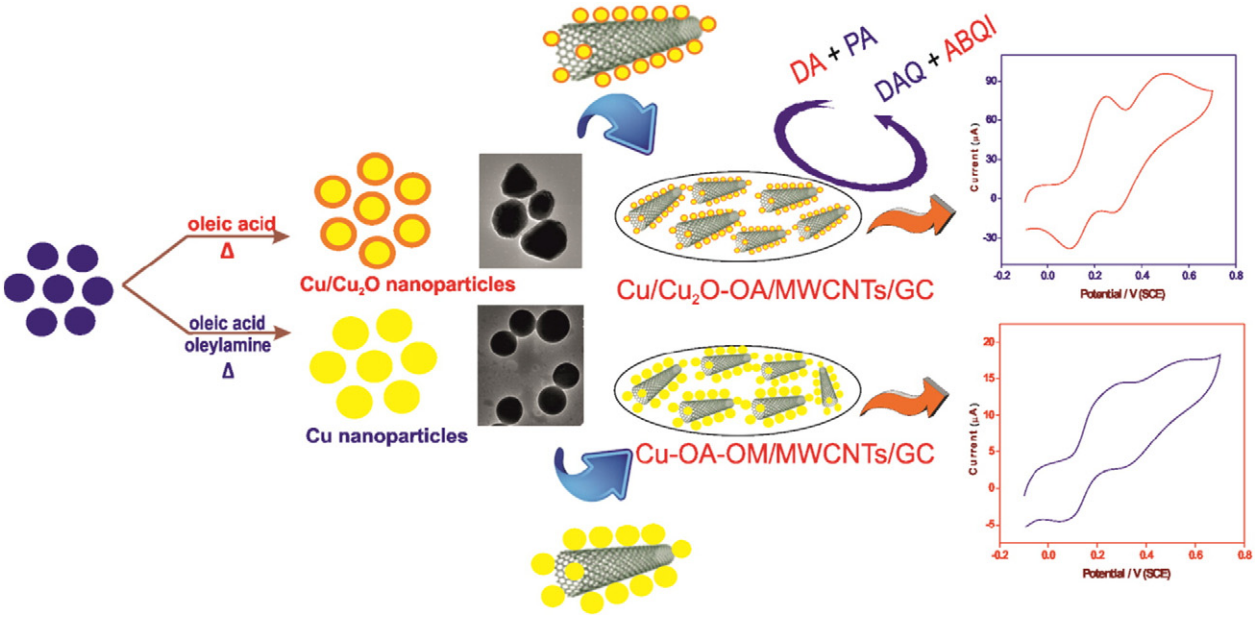

Scheme 2. Schematic representation of Cu/Cu_2O-OA/MWCNTs/GC and Cu-OA-OM/MWCNTs/GC modified electrode in the presence of paracetamol and dopamine simultaneously.

and it is in accordance with the following linear regression equation:

$$\log(I_{pa}) = 0.760 + 0.62\log(\nu)\ (V/s), R^2 = 0.998 \quad (2)$$

It is however interesting with increase in scan rate, the oxidation and reduction peak potentials tend to get shifted to more anodic and cathodic regions and at the same time peak potential separation (ΔEp)

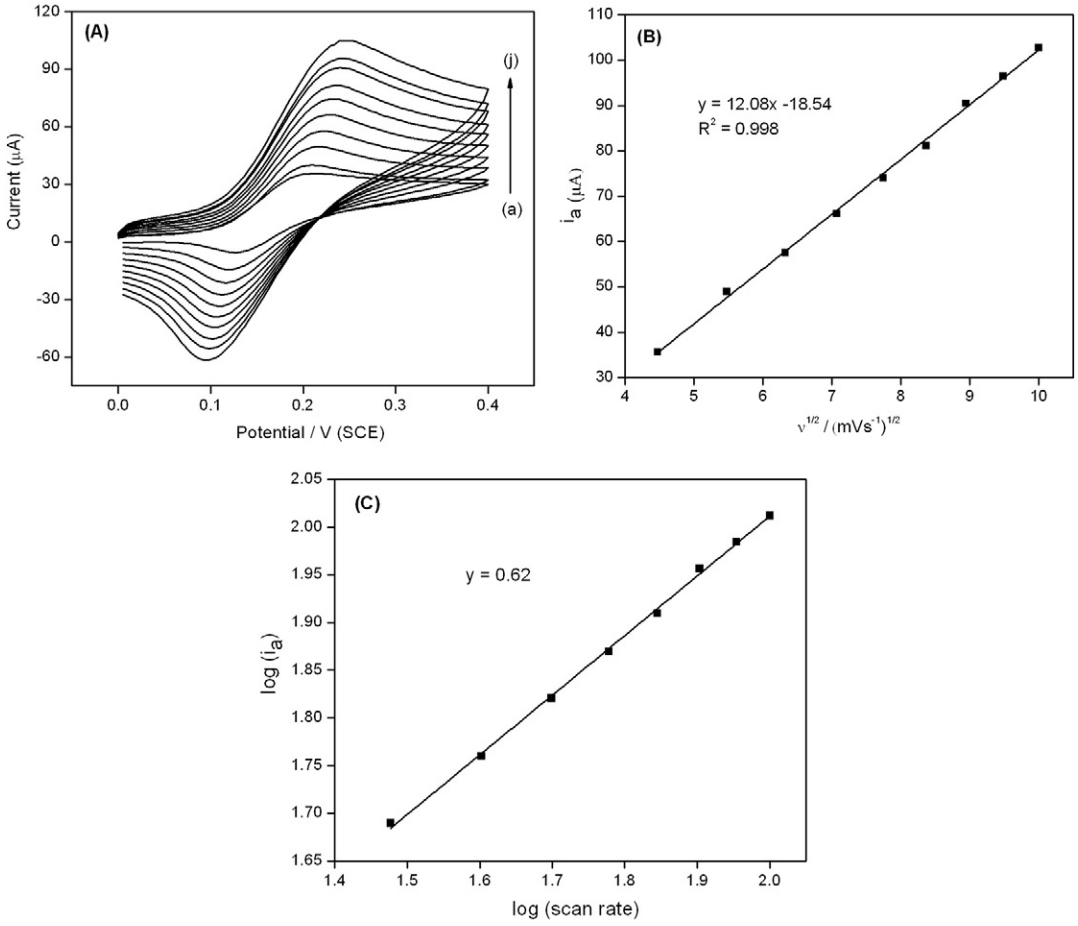

Fig. 7. (A) CVs of Cu/Cu_2O-OA/MWCNTs modified GC electrode in 0.1 mM dopamine (0.1 M PBS -pH 7.0) at different scan rates (from inner to outer) of (a) 10, (b) 20, (c) 30, (d) 40, (e) 50, (f) 60, (g) 70, (h) 80, (i) 90 and (j) 100 mV s^{-1}. (B) Calibration plot of square root of scan rate *vs.* anodic peak current of dopamine. (C) Calibration plot of $\log(i_a)$ and $\log(\nu)$.

value also seems to be greater than the theoretical expected value of 0.059/ΔEp indicating that electron transfer process for dopamine at Cu/Cu_2O-OA/MWCNTs modified electrode is quasi-reversible. The number of electrons involved in the electrochemical oxidation of dopamine can be calculated as two as earlier reported [57,58].

The charge transfer rate coefficient (α) and apparent charge transfer rate constant (k_s) for electron transfer between the electrode and the redox couple can be determined using Laviron equation [59]. A linear relationship was obtained by varying the anodic peak potential to the logarithm of scan rate (log ν) yields a slope equal to $2.303RT / (1 - \alpha)nF$ (where, F is the Faraday constant, R the gas constant and T is the absolute temperature), the value of α was calculated to be 0.73. According to Laviron theory [59], the peak potential separation was less than 200 mV, therefore the apparent electron transfer rate constant can be calculated using $k_s = mnF\nu / RT$, where m is the parameter related to peak potential separation, n the number of electrons involved in the reaction, ν is the scan rate and all other symbols have their usual meanings. Therefore the k_s value of 1.29 s^{-1} was obtained for Cu/Cu_2O-OA/MWCNTs modified GC electrode signifies that presence of Cu/Cu_2O nanoparticles on the electrode surface promote the electron transfer between solution and the electrode surface. Sharp et al. [60] used a simple and approximate method for the determination of surface concentration (Γ) of the electrochemical species on the modified electrode using the equation $I_p = n^2F^2A\Gamma\nu / 4RT$. Where A is the electrode surface area (0.0707 cm^2) and n, F, ν, R, T has their common meanings. From the slope of the linear relationship between peak potential and scan rate the surface concentration of Cu/Cu_2O-OA/MWCNTs modified GC electrode can be calculated as 2.833×10^{-6} mol/cm^2.

3.8. Differential pulse voltammetric determination of paracetamol and dopamine

The utilization of novel Cu/Cu_2O-OA/MWCNTs modified GC electrode for the simultaneous determination of dopamine and paracetamol using DPV is shown in Fig. 8. For DPVs, the potential waveform was optimized with respect to the simultaneous determination of dopamine and paracetamol: pulse amplitude 50 mV, with scan rate 20 mV s^{-1}. It is very interesting when we determine simultaneously by increasing both the concentrations of dopamine and paracetamol. Fig. 8A shows that the DPVs (baseline corrected) response for the simultaneous determination of dopamine and paracetamol with well-distinguished peaks at potential 150 mV and 350 mV, corresponding to the oxidation of dopamine and paracetamol. With increasing concentrations of dopamine and paracetamol, the peak currents increase linearly with a peak separation value of 200 mV, and hence the obtained high peak-peak separation value is large enough for the simultaneous determination. The appearance of sharp peak along with increase in peak current gradually with increase in the concentration of paracetamol and dopamine, which reflects that Cu/Cu_2O-OA/MWCNTs modified GC electrode is not affected by any interfering species. As shown in Fig. 8B the electrochemical response of dopamine is linear at low concentration ranging from 0.02 μM to 0.159 μM. The first linear equation can be expressed as: I_{pa} (μA) =

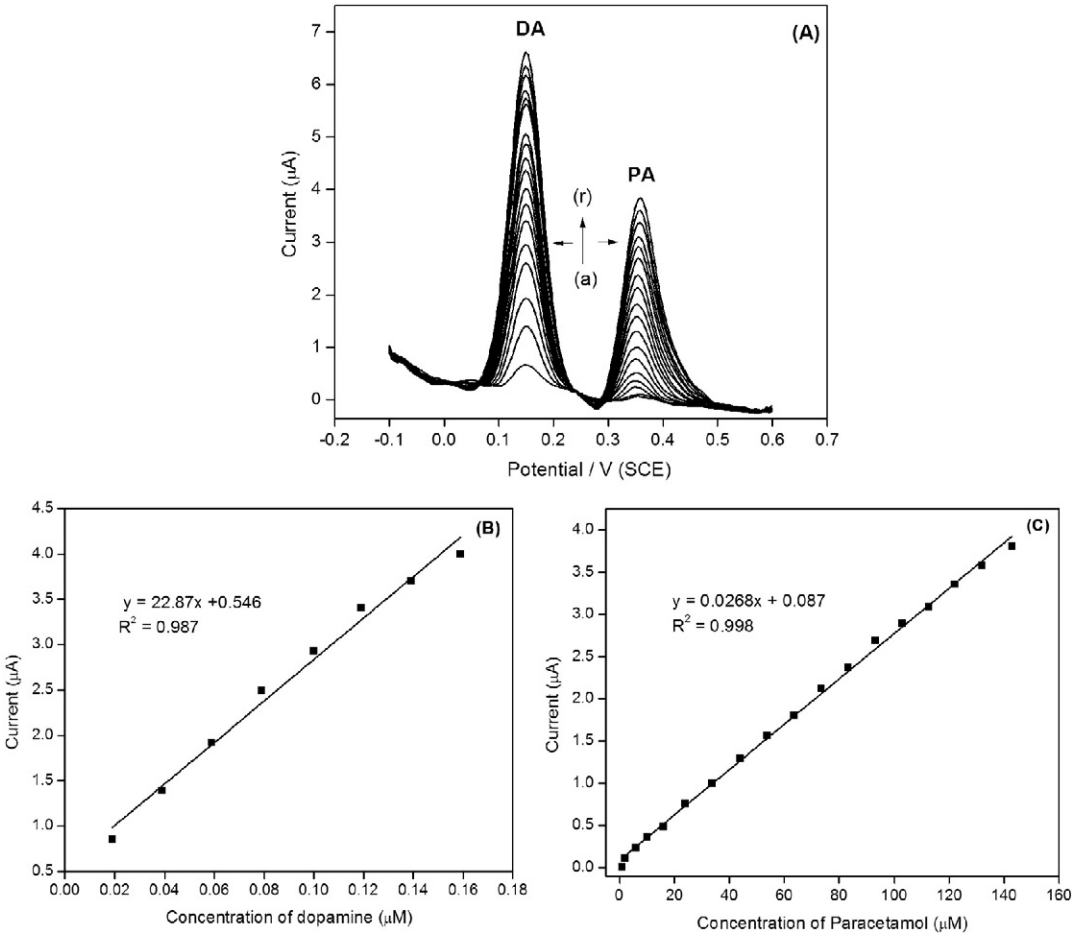

Fig. 8. (A) DPVs (baseline corrected) of Cu/MWCNTs modified GC electrode in 0.1 M PBS (pH 7.0) with scan rate 20 mV s^{-1} and pulse amplitude 50 mV containing increasing concentration of mixture of dopamine (a) 0.02 μM, (b) 0.04 μM, (c) 0.06 μM, (d) 0.08 μM, (e) 0.1 μM, (f) 0.119 μM, (g) 0.139 μM, (h) 0.159 μM, (i) 0.179 μM, (j) 0.2 μM, (k) 0.239 μM, (l) 0.299 μM, (m) 0.379 μM, (n) 0.459, (o) 0.599 μM, (p) 0.739 μM, (q) 0.879 and (r) 1.07 μM and paracetamol (a) 1 μM, (b) 2 μM, (c) 5.9 μM, (d) 10 μM, (e) 15.9 μM, (f) 23.9 μM, (g) 33.8 μM, (h) 43.8 μM, (i) 53.7 μM, (j) 63.5 μM, (k) 73.4 μM, (l) 83.3 μM, (m) 93.1 μM, (n) 102.9 μM, (o) 112.7 μM, (p) 122 μM, (q) 132 μM and (r) 142.9 μM. (B) Calibration plot for increasing concentration of dopamine *vs.* peak current. (C) Calibration plot for increasing concentration of paracetamol *vs.* peak current.

0.546 + 22.87 (concentration of dopamine) (μM); $R^2 = 0.989$. The corresponding sensitivity was obtained as 22.87 μA/μM with a detection limit (3σ) of 3.27 nM (S/N = 3). Whereas in case of paracetamol (Fig. 8C) Cu/Cu_2O-OA/MWCNTs modified GC electrode shows a linear calibration plot, throughout with increasing concentrations of paracetamol ranging from 1 μM to 142.9 μM and the linear equation can be written as I_{pa} (μA) = 0.087 + 0.026 (concentration of paracetamol) (μM); $R^2 = 0.998$. The sensitivity was obtained as 0.026 μA/μM with a detection limit (3σ) of 1.51 μM (S/N = 3). As observed from Table 2 and 3 (SI-2), the obtained linear range, detection limit and peak potential for the determination of dopamine and paracetamol at Cu/Cu_2O-OA/MWCNTs/GC modified electrode are comparable with the recently reported literatures.

3.9. Effect of interferences, stability and reproducibility

The effect of interferences on the simultaneous determination of dopamine and paracetamol was investigated on Cu/Cu_2O-OA/MWCNTs/GC modified electrode in presence of higher concentration (2.5 mM) of ascorbic acid. As can be seen from Fig. 9 addition of interfering species like ascorbic acid into the reacting mixture solution containing dopamine and paracetamol experiences a positive shift for the oxidation of ascorbic acid. The oxidation peak potential of ascorbic acid appeared at −0.14 V which signifies that Cu/Cu_2O-OA/MWCNTs/GC modified electrode does not interfere with the current response in presence of dopamine and paracetamol.

Thus results suggest that Cu/Cu_2O-OA/MWCNTs/GC modified electrode modified electrode has high sensitivity and good reproducibility for the determination of dopamine and paracetamol. The reproducibility of the Cu/Cu_2O-OA/MWCNTs modified GC electrode was evaluated by the precision, which was obtained by repeating six measurements in the same solution containing 2 μM dopamine. A relative standard deviation (RSD) of 1.39% was obtained for six successive measurements, indicating that the Cu/Cu_2O-OA/MWCNTs modified GC electrode is not subjected to surface fouling by the oxidation products.

3.10. Analytical applications

The applicability of the proposed Cu/Cu_2O-OA/MWCNTs modified GC electrode was validated for the determination of dopamine and paracetamol in pharmaceutical [DOLOPAR (paracetamol 500 mg + caffeine 25 mg); DOPAMINE (dopamine hydrochloride 200 mg/5 mL)] samples. The paracetamol tablets of labeled value was accurately weighed and ground to a fine powder using mortar and the content of the sample was diluted to obtain the concentration of paracetamol in the working range. From that, a portion of the sample was added into the electrochemical cell containing 0.1 M PBS. DOPAMINE i/v solution was diluted to 100 times with 0.1 M PBS, and these diluted samples were injected to electrochemical cell containing 0.1 M PBS and then the DPV measurements were recorded for oxidation of dopamine and paracetamol. The concentration of dopamine and paracetamol in the pharmaceutical samples was calculated from the standard calibration plot. The recovery result shows a satisfactory remark between the labeled analytical content and the determined value. The recovery values obtained is effective and can be applied for determination of dopamine and paracetamol in commercial samples, which suggests that proposed method could be effectively used for simultaneous determination of dopamine paracetamol in practical applications.

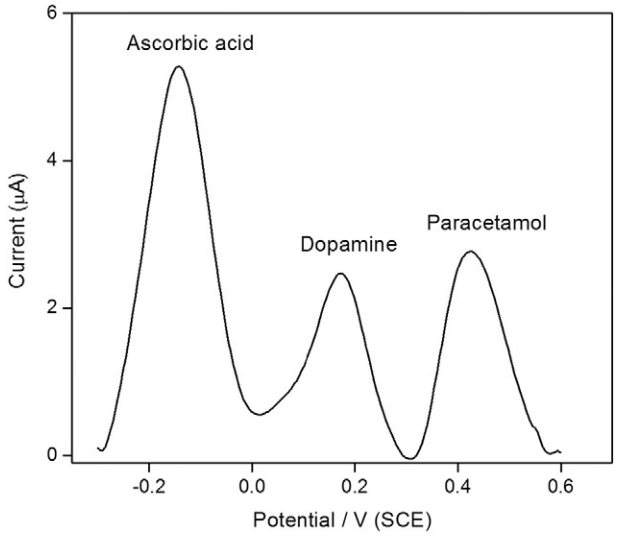

Fig. 9. DPV interfering response of Cu/Cu_2O-OA/MWCNTs/GC modified electrode in presence of ascorbic acid, dopamine and paracetamol containing 0.1 M PBS.

4. Conclusions

In conclusion, a convenient successful route adopted for the synthesis of Cu nanoparticles using oleic acid and oleylamine *via* a thermal decomposition method. This method takes advantage over other methods for the synthesis of monodisperse Cu nanoparticles of well-defined shape and size. From XRD analysis, it confirms the formation of high purity Cu nanoparticles with single phase crystalline and XPS also evidences the formation of pure Cu only. The sole use of oleic acid stabilized nanoparticles was also prepared in order to evaluate the formation of surface oxidation of Cu nanoparticles in presence of oleic acid. Also we compared the electrochemical properties of two types of nanoparticles obtained from oleic acid and also from combination of oleic acid and oleylamine. The advantage of Cu/Cu_2O nanoparticles obtained from oleic acid alone are homogeneously dispersed in ethanol which provide high electron transfer ability with enhanced electrochemical reversibility and large oxidation peak separation for simultaneous determination of dopamine and paracetamol when compared to Cu nanoparticles obtained by combination of oleic acid and oleylamine. Therefore we believe that, presence of metal oxide on surface of metal nanoparticles on modified electrode surface will offer higher electrochemical performance indicating a great promising material for a wide range of analytical applications.

Acknowledgements

The authors gratefully acknowledge Department of Science and Technology (DST-PURSE) for the financial support and National Centre for Nanoscience and Nanotechnology (NCNSNT) for HRTEM and XPS measurements.

Appendix A. Supplementary data

Supplementary data to this article can be found online at http://dx.doi.org/10.1016/j.molliq.2016.06.028.

References

[1] F.R. Xiu, F.S. Zhang, Size-controlled preparation of Cu_2O nanoparticles from waste printed circuit boards by supercritical water combined with electrokinetic process, J. Hazard. Mater. 233 (2012) 200–206.
[2] H. Lee, S.W. Yoon, E.J. Kim, J. Park, In-situ growth of copper sulfide nanocrystals on multiwalled carbon nanotubes and their application as novel solar cell and amperometric glucose sensor materials, Nano Lett. 7 (2007) 778–784.
[3] M.I. Awad, T. Ohsaka, An electrocatalytic oxygen reduction by copper nanoparticles modified Au(100)-rich polycrystalline gold electrode in 0.5 M KOH, J. Power Sources 226 (2013) 306–312.
[4] Y. Li, W. Lu, Q. Huang, C. Li, W. Chen, Copper sulfide nanoparticles for photothermal ablation of tumor cells, Nanomedicine 5 (2010) 1161–1171.
[5] G.H. Chan, J. Zhao, E.M. Hicks, G.C. Schatz, R.P. Van Duyne, Plasmonic properties of copper nanoparticles fabricated by nanosphere lithography, Nano Lett. 7 (2007) 1947–1952.

[6] J.P. Cason, C.B. Roberts, Metallic copper nanoparticle synthesis in AOT reverse micelles in compressed propane and supercritical ethane solutions, J. Phys. Chem. B 104 (2000) 1217–1221.
[7] H. Ohde, F. Hunt, C.M. Wai, Synthesis of silver and copper nanoparticles in a water-in-supercritical-carbon dioxide microemulsion, Chem. Mater. 13 (2001) 4130–4135.
[8] R.V. Kumar, R. Elgamiel, Y. Diamant, A. Gedanken, Sonochemical preparation and characterization of nanocrystalline copper oxide embedded in poly(vinyl alcohol) and its effect on crystal growth of copper oxide, Langmuir 17 (2001) 1406–1410.
[9] M.T. Swihart, Vapor-phase synthesis of nanoparticles, Curr. Opin. Colloid Interface Sci. 8 (2003) 127–133.
[10] A. Henglein, Formation and absorption spectrum of copper nanoparticles from the radiolytic reduction of $Cu(CN)_2^-$, J. Phys. Chem. B 104 (2000) 1206–1211.
[11] Y. Shimotsuma, T. Yuasa, H. Homma, M. Sakakura, A. Nakao, K. Miura, K. Hirao, M. Kawasaki, J. Qiu, P.G. Kazansky, Photoconversion of copper flakes to nanowires with ultrashort pulse laser irradiation, Chem. Mater. 19 (2007) 1206–1208.
[12] A. Radi, D. Pradhan, Y. Sohn, K.T. Leung, Nanoscale shape and size control of cubic, cuboctahedral, and octahedral Cu–Cu_2O core–shell nanoparticles on Si(100) by one-step, templateless, capping-agent-free electrodeposition, ACS Nano 4 (2010) 1553–1560.
[13] B.K. Park, S. Jeong, D. Kim, J. Moon, S. Lim, J.S. Kim, Synthesis and size control of monodisperse copper nanoparticles by polyol method, J. Colloid Interface Sci. 311 (2007) 417–424.
[14] D.E. Diaz-Droguett, R. Espinoza, V.M. Fuenzalida, Copper nanoparticles grown under hydrogen: study of the surface oxide, Appl. Surf. Sci. 257 (2011) 4597–4602.
[15] P. Lignier, R. Bellabarba, R.P. Tooze, Scalable strategies for the synthesis of well-defined copper metal and oxide nanocrystals, Chem. Soc. Rev. 41 (2012) 1708–1720.
[16] J.J. Brege, C.E. Hamilton, C.A. Crouse, A.R. Barron, Ultrasmall copper nanoparticles from a hydrophobically immobilized surfactant template, Nano Lett. 9 (2009) 2239–2242.
[17] M. Lattuada, T.A. Hatton, Functionalization of monodisperse magnetic nanoparticles, Langmuir 23 (2007) 2158–2168.
[18] J. Park, K. Aan, Y. Hwang, J.G. Park, H.J. Noh, J.Y. Kim, J.H. Park, N.M. Hwang, T. Hyeon, Ultra-large-scale syntheses of monodisperse nanocrystals, Nat. Mater. 3 (2004) 891–895.
[19] D. Mott, J. Galkowski, L. Wang, J. Luo, C.J. Zhong, Synthesis of size-controlled and shaped copper nanoparticles, Langmuir 23 (2007) 5740–5745.
[20] S. Sun, C.B. Murray, D. Weller, L. Folks, A. Moser, Monodisperse FePt nanoparticles and ferromagnetic FePt nanocrystal superlattices, Science 287 (2000) 1989–1992.
[21] N. Wu, L. Fu, M. Su, M. Aslam, K.C. Wong, V.P. Dravid, Interaction of fatty acid monolayers with cobalt nanoparticles, Nano Lett. 4 (2004) 383–386.
[22] C. Wang, D. van der Vliet, K.L. More, N.J. Zaluzec, S. Peng, S. Sun, H. Daimon, G. Wang, J. Greeley, J. Pearson, A.P. Paulikas, G. Karapetrov, D. Strmcnik, N.M. Markovic, V.R. Stamenkovic, Multimetallic Au/$FePt_3$ nanoparticles as highly durable electrocatalyst, Nano Lett. 11 (2011) 919–926.
[23] H. Zeng, P.M. Rice, S.X. Wang, S. Sun, Shape-controlled synthesis and shape-induced texture of MnFe2O4 nanoparticles, J. Am. Chem. Soc. 126 (2004) 11458–11459.
[24] B. Habibi, M. Jahanbakhshi, M.H. Pournaghi-Azar, Simultaneous determination of acetaminophen and dopamine using SWCNT modified carbon–ceramic electrode by differential pulse voltammetry, Electrochim. Acta 56 (2011) 2888–2894.
[25] G.P. Keeley, N. McEvoy, H. Nolan, S. Kumar, E. Rezvani, M. Holzinger, S. Cosnier, G.S. Duesberg, Simultaneous electrochemical determination of dopamine and paracetamol based on thin pyrolytic carbon films, Anal. Methods 4 (2012) 2048–2053.
[26] N.F. Atta, A. Galal, F.M. Abu-Attia, S.M. Azab, Simultaneous determination of paracetamol and neurotransmitters in biological fluids using a carbon paste sensor modified with gold nanoparticles, J. Mater. Chem. 21 (2011) 13015–13024.
[27] S.A. Kumar, C.F. Tang, S.M. Chen, Electroanalytical determination of acetaminophen using nano-TiO_2/polymer coated electrode in the presence of dopamine, Talanta 76 (2008) 997–1005.
[28] N.F. Atta, M.F. El-Kady, Poly(3-methylthiophene)/palladium sub-micro-modified sensor electrode. Part II: voltammetric and EIS studies, and analysis of catecholamine neurotransmitters, ascorbic acid and acetaminophen, Talanta 79 (2009) 639–647.
[29] Z.A. Alothman, N. Bukhari, S.M. Wabaidur, S. Haider, Simultaneous electrochemical determination of dopamine and acetaminophen using multiwall carbon nanotubes modified glassy carbon electrode, Sensors Actuators B Chem. 146 (2010) 314–320.
[30] W. Wei, Y. Lu, W. Chen, S. Chen, One-pot synthesis, photoluminescence, and electrocatalytic properties of subnanometer-sized copper clusters, J. Am. Chem. Soc. 133 (2011) 2060–2063.
[31] D. Tasis, N. Tagmatarchis, V. Georgakilas, M. Prato, Soluble carbon nanotubes, Chem. Eur. J. 9 (2003) 4000–4008.
[32] J.F. Moulder, W.F. Stickle, P.E. Sobol, K.D. Bomben, Handbook of X-ray Photoelectron Spectroscopy, ULVAC-PHI, Inc., Japan, 1995.
[33] Y.C. Tsai, S.C. Li, J.M. Chen, Cast thin film biosensor design based on a nafion backbone, a multiwalled carbon nanotube conduit, and a glucose oxidase function, Langmuir 21 (2005) 3653–3658.
[34] M. Shi, H.S. Kwon, Z. Peng, A. Elder, H. Yang, Effects of surface chemistry on the generation of reactive oxygen species by copper nanoparticles, ACS Nano 6 (2012) 2157–2164.
[35] Z. Ai, L. Zhang, S. Lee, W. Ho, Interfacial hydrothermal synthesis of Cu@Cu_2O core–shell microspheres with enhanced visible-light-driven photocatalytic activity, J. Phys. Chem. C 113 (2009) 20896–20902.
[36] M. Devaraj, R.K. Deivasigamani, S. Jeyadevan, Colloids Surf, B: Biointerfaces 102 (2013) 554–561.
[37] T. Ghodselahi, M.A. Vesaghi, A. Shafiekhani, A. Baghizadeh, M. Lameii, XPS study of the Cu@Cu_2O core-shell nanoparticles, Appl. Surf. Sci. 255 (2008) 2730–2734.
[38] G.S. Chaubey, C. Barcena, N. Poudyal, C. Rong, J. Gao, S. Sun, J.P. Liu, Synthesis and stabilization of FeCo nanoparticles, J. Am. Chem. Soc. 129 (2007) 7214–7215.
[39] R. Si, Y.W. Zhang, L.P. You, C.H. Yan, Rare-earth oxide nanopolyhedra, nanoplates, and nanodisks, Angew. Chem. Int. Ed. 44 (2005) 3256–3260.
[40] G. Krylova, L.J. Giovanetti, F.G. Requejo, N.M. Dimitrijevic, A. Prakapenka, E.V. Shevchenko, Study of nucleation and growth mechanism of the metallic nanodumbbells, J. Am. Chem. Soc. 134 (2012) 4384–4392.
[41] V. Nandwana, K.E. Elkins, N. Poudyal, G.S. Chaubey, K. Yano, J.P. Liu, Size and shape control of monodisperse FePt nanoparticles, J. Phys. Chem. C 111 (2007) 4185–4189.
[42] Y. Wang, J.F. Wong, X. Teng, X.Z. Lin, H. Yang, "Pulling" nanoparticles into water: phase transfer of oleic acid stabilized monodisperse nanoparticles into aqueous solutions of α-cyclodextrin, Nano Lett. 3 (2003) 1555–1559.
[43] C.R. De Silva, S. Smith, I. Shim, J. Pyun, T. Gutu, J. Jiao, Z. Zheng, Lanthanide(III)-doped magnetite nanoparticles, J. Am. Chem. Soc. 131 (2009) 6336–6337.
[44] A.H. Latham, M.J. Wilson, P. Schiffer, M.E. Williams, TEM-induced structural evolution in amorphous Fe oxide nanoparticles, J. Am. Chem. Soc. 128 (2006) 12632–12633.
[45] S. Sun, H. Zeng, D.B. Robinson, S. Raoux, P.M. Rice, S.X. Wang, G. Li, Monodisperse MFe_2O_4 (M = Fe, Co, Mn) nanoparticles, J. Am. Chem. Soc. 126 (2004) 273–279.
[46] W. Bu, Z. Chen, F. Chen, J. Shi, Oleic acid/oleylamine cooperative-controlled crystallization mechanism for monodisperse tetragonal bipyramid $NaLa(MoO_4)_2$ nanocrystals, J. Phys. Chem. C 113 (2009) 12176–12185.
[47] N. Zheng, J. Fan, G.D. Stucky, One-step one-phase synthesis of monodisperse noblemetallic nanoparticles and their colloidal crystals, J. Am. Chem. Soc. 128 (2006) 6550–6551.
[48] M. Chen, J. Kim, J.P. Liu, H. Fan, S. Sun, Synthesis of FePt nanocubes and their oriented self-assembly, J. Am. Chem. Soc. 128 (2006) 7132–7133.
[49] Y. Li, J. Liu, Y. Wang, Z.L. Wang, Preparation of monodispersed Fe–Mo nanoparticles as the catalyst for CVD synthesis of carbon nanotubes, Chem. Mater. 13 (2001) 1008–1014.
[50] N. Shukla, C. Liu, P.M. Jones, D. Weller, FTIR study of surfactant bonding to FePt nanoparticles, J. Magn. Magn. Mater. 266 (2003) 178–184.
[51] H.G. Bagaria, E.T. Ada, M. Shamsuzzoha, D.E. Nikles, D.T. Johnson, Understanding mercapto ligand exchange on the surface of FePt nanoparticles, Langmuir 22 (2006) 7732–7737.
[52] S. Brillians Revin, S. Abraham John, Electrochemical sensor for neurotransmitters at physiological pH using a heterocyclic conducting polymer modified electrode, Analyst 137 (2012) 209–215.
[53] M. Boopathi, M.S. Won, Y.B. Shima, A sensor for acetaminophen in a blood medium using a Cu(II)-conducting polymer complex modified electrode, Anal. Chim. Acta 512 (2004) 191–197.
[54] N.F. Atta, M.F. El-Kady, A. Galal, Simultaneous determination of catecholamines, uric acid and ascorbic acid at physiological levels using poly(*N*-methylpyrrole)/Pd-nanoclusters sensor, Anal. Biochem. 400 (2010) 78–88.
[55] M. Devaraj, R.K. Deivasigamani, S. Jayadevan, Anal. Methods 5 (2013) 3503–3515.
[56] N.F. Atta, A. Galal, R.A. Ahmed, Simultaneous determination of catecholamines and serotonin on poly(3,4-ethylene dioxythiophene) modified Pt electrode in presence of sodium dodecyl sulfate, J. Electrochem. Soc. 158 (2011) F52–F60.
[57] A. Ciszewski, G. Milczarek, Polyeugenol-modified platinum electrode for selective detection of dopamine in the presence of ascorbic acid, Anal. Chem. 71 (1999) 1055–1061.
[58] D. Yuan, X. Yuan, S. Zhou, W. Zou, T. Zhou, *N*-doped carbon nanorods as ultrasensitive electrochemical sensors for the determination of dopamine, RSC Adv. 2 (2012) 8157–8163.
[59] E. Laviron, General expression of the linear potential sweep voltammogram in the case of diffusionless electrochemical systems, J. Electroanal. Chem. 101 (1979) 19–28.
[60] M. Sharp, M. Petersson, K. Edstrom, Preliminary determinations of electron transfer kinetics involving ferrocene covalently attached to a platinum surface, J. Electroanal. Chem. 95 (1979) 123–130.